vibration

MDPI

Article

Finite Element Analysis of *Coffea arabica* L. var. Colombia Fruits for Selective Detachment Using Forced Vibrations

Hector A. Tinoco [1,2,*] and Fabio M. Peña [1]

[1] Experimental and Computational Mechanics Laboratory, Universidad Autónoma de Manizales, Antigua Estación del Ferrocarril, Edificio Sacatín C.P., Manizales 17 0001, Colombia; fabiope@autonoma.edu.co

[2] Institute of Physics of Materials, Czech Academy of Sciences, Zizkova 22, Brno 616 62, Czech Republic

* Correspondence: htinoco@autonoma.edu.co; Tel.: +57-6872-7211

Received: 28 June 2018; Accepted: 13 September 2018; Published: 18 September 2018

Abstract: This study provides a forced vibration analysis to evaluate the stresses at the pedicel interfaces of the fruit-peduncle system of *Coffea arabica* L. var. Colombia by means of finite element analysis. The real topology of the fruit-peduncle system was developed from a proposed numerical procedure to complete a dynamic analysis. The Young's modulus of the fruit was approximated from firmness indices for all stages of ripening. Numerical computations were performed in the frequency range of 0 to 400 Hz and three vibration modes were identified in this bandwidth. Results show that the second natural frequency (128 Hz) is acceptable for stimulating the detachment of ripe fruits because the fruit-pedicel-peduncle system induces bending in the fruit interface. As a final conclusion, we determine that dynamic excitations between 120 and 150 Hz could permit selective stimulus of ripe fruits, since other ripening stages were not stimulated in this frequency range.

Keywords: vibration analysis; coffee fruits; selective harvesting; *Coffea arabica*; finite element analysis

1. Introduction

The coffee tree is a tropical evergreen that grows in regions between the tropics of Cancer and Capricorn between 700 and 2000 m above mean sea level [1]. The coffee fruit is a green small fruit of irregular geometry that is bitter when unripe and sweet when ripe. Colombian coffee and its sub-products are internationally recognized for the excellent quality, from which the profits generate a considerable socio-economic impact in the producer regions [2]. Coffee fruits are harvested manually by hand-picking ripe fruits one by one. Manual gathering means less than 2.5% of green fruits can be harvested in Colombia [3]. The harvesting stage is the most expensive and complex of the coffee production process in Colombia. Therefore, there is an interest in studying diverse methods of selectively harvesting ripe coffee fruits.

The direct mechanization in the harvesting of fruits has helped reduce production costs as well as increase the productivity in the harvesting process. Different technologies have been implemented with success in fruits such as apples, peaches, cherries, and olives [4–6]. These have overcome limitations such as topography, spatial distribution of the crop, relation between weight and detachment force, etc. A fundamental principle should be applied in mechanized harvesting to achieve the selective detachment of fruits by vibration. It involves transmitting motion to the fruits until the inertial force exceeds the bonding strength between the fruit and the pedicel-peduncle interface [7]. However, the challenge is more complicated if only ripe fruits should be selectively detached. In the last decades, mechanical harvesting has played an important role in the coffee production chain [8,9], since the mechanization process depends on the geographic variability of the crop, fruit selectivity,

damage to the plants, and so on. For example, in Colombia coffee crops usually found in mountainous terrains, the harvesting is performed year-round as plants cannot be damaged and only ripe fruits must be harvested. These aspects mean that the mechanization cannot be implemented with success, as in Brazil [10].

Different vibratory devices have been designed and implemented on the trunk or branches of the tree [11,12]. However, harvesting by mechanical vibration requires a knowledge of the mechanical parameters involved in the detachment of fruits, including those related to the natural frequencies, motion amplitude, and application of the vibration time [10]. Determination of these parameters permits obtaining better performance in the detachment of ripe fruits, as well as diminishes the impact of the motions over the tree. As such, the mechanical properties of the subsystems (i.e., fruit-peduncle) of the tree should be studied to describe their dynamic behavior. It is more feasible from a dynamic point of view to characterize the fruit-peduncle interface since it has small topological differences with respect to the geometry of the trees [13–16].

Vibration frequencies and their performance on selective harvesting have been studied experimentally [11,17–19]. Different frequency intervals were established experimentally to stimulate selective harvesting, but these intervals were determined without characterizing the sub-systems. Recently, the efficiency of fruit detachment from coffee plants subjected to mechanical vibrations was studied [20]. These tests combined different frequencies, which were 16.4 Hz, 20.3 Hz, 24 Hz, 25.6 Hz, 30.0 Hz, and 33.0 Hz. Results showed low selective performance in the detachment of ripe fruits compared with the detached unripe fruits. This means that the modal parameters of the sub-systems (fruit peduncle) should be studied in detail to concentrate the energy of the vibration on the ripe fruits. It is important to understand the detachment mechanisms of ripe fruits, since experimental studies have not had success when the tree itself was stimulated. This is seen an opportunity to comprehend the dynamics of the coffee fruits, since vibrations in inadequate frequencies could damage the trunk, defoliate the tree, and detach unripe fruits.

Recently, numerical simulations were performed to determine the frequency intervals at which the fruit system can be excited with vibration. For example, a modal analysis for determining the vibration modes of coffee fruits was realized [14]. However, in this study, the mechanical properties of the fruit were not defined clearly. A complementary modal analysis on the fruit peduncle system was performed by Tinoco et al. [15] to identify natural frequencies with its respective associated vibration modes. The study showed convergence in the determination of natural frequencies, which were called selective frequencies. These showed significant differences between the different ripening stages. Specifically, the differences were demarked with fruits in incomplete ripening stages. To achieve the simulations, the mechanical and geometrical properties of the fruit were obtained with numerical procedures combined with experimental data. The natural frequencies and modal shapes of the fruit-stem-branch system were computed by applying a stochastic finite element method which was performed by Coelho et al. [21]. The elastic modulus and the specific mass were treated as random variables in the simulation. Therefore, the natural frequencies were determined as a function of the mechanical properties, including its variability. The study performed by Tinoco et al. [22] showed a harmonic finite element analysis of a glomerulus of three fruits in different ripening stages that were combined in four groups of fruits. Applying a chirp force signal verified which fruit could be detached based on an experimental detachment model. Results indicated that dynamic excitations applied in between 130 to 150 Hz detached only ripe fruits.

The aim of this study was to analyze the stresses generated at the pedicel-fruit and pedicel-peduncle interfaces by means of forced vibrations using finite element analysis. The topology of the fruit (computer aided design (CAD) models) was reproduced applying the methodology reported by Tinoco et al. [15]. Additionally, an estimation of the Young's modulus is proposed from an analytical equation to the semi-experimental data of elasticity obtained by Tinoco [19].

2. Geometric Model for the Fruit *Coffea arabica* L. var. Colombia [15]

Coffea arabica L. var. Colombia fruits can be represented from anthesis until maturation by a computer model established by Tinoco et al. [15] which can describe the growth from an initial volume V_i until a posterior volume V_{i+1}. Figure 1 shows a fruit oriented at the three directions defined by the unitary vectors e_1, e_2 and e_3, which define the shape in each stage of ripening, where e_1 and e_2 are equatorial directions for the diameters ϕ_1 and ϕ_2, respectively, such that $\phi_1 \geq \phi_2$. ϕ_3 is the polar diameter in the e_3 direction, orthogonal to the plane $e_1 - e_2$. Diameter ϕ_1 is the highest diameter in this plane, which consequently defines e_1. The directions e_1, e_2 and e_3 are orthogonal by definition. Orthogonal diameters are variables that depend on the ripening time [23], and the hyperplanes established by $e_1 - e_2$, $e_3 - e_1$ and $e_2 - e_3$ are symmetric planes in the fruit, as demonstrated by Tinoco et al. [15].

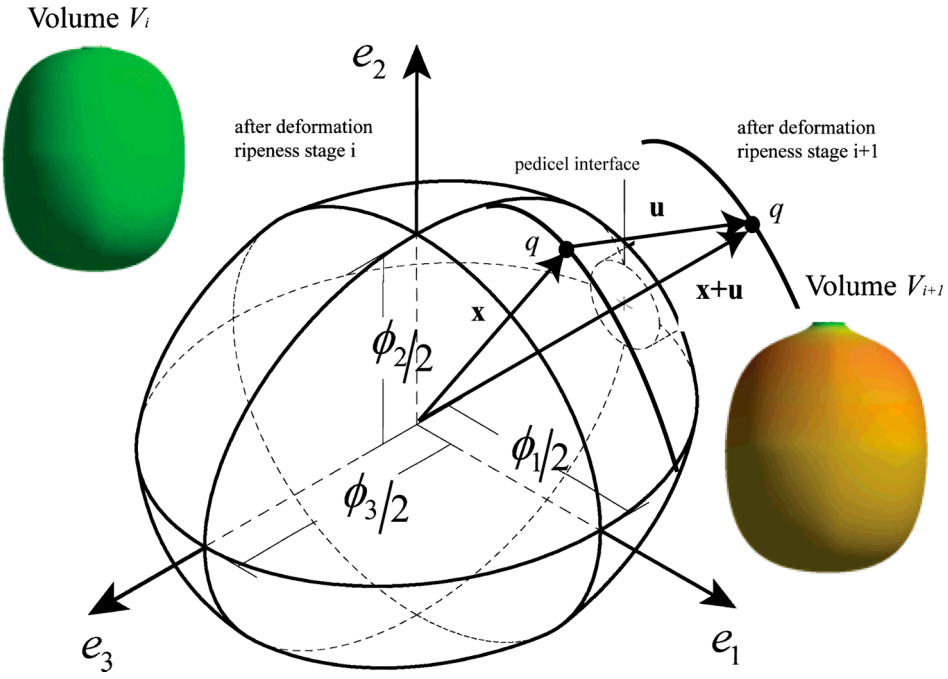

Figure 1. Coffee fruit model.

A set of equations $f_i(t), \forall i = 1, 2, 3$, dependent on the time, represent one-eighth of the fruit. This is limited by the planes $e_k - e_j, \forall kj = 12, 23, 31$, as illustrated in Figure 2. Bezier cubic functions are established as functions for the set $f_i(t)$. Each boundary is constructed from the control points ${P_1}^{e_k - e_j}$, ${P_2}^{e_k - e_j}$, ${P_3}^{e_k - e_j}$ and ${P_4}^{e_k - e_j}$ determined for each plane $e_k - e_j$. These functions describe the shape in each eighth by means of the following calculation:

$$f_i^k(t) = \left\{ (\mathbf{X}_i(t), \mathbf{Y}_i(t)) \in \mathbb{R}^2 \middle| \mathbf{X}_i(t) = {\mathbf{a}_i}^{\mathbf{T}}\mathbf{t},\ \mathbf{Y}_i(t) = {\mathbf{b}_i}^{\mathbf{T}}\mathbf{t},\ \forall t \in (0,1) \right\}, \forall k = 1, \ldots, 4 \quad (1)$$

where ${\mathbf{a}_i}^{\mathbf{T}} = \begin{bmatrix} a_{1i} & a_{2i} & a_{3i} & a_{4i} \end{bmatrix}$, ${\mathbf{b}_i}^{\mathbf{T}} = \begin{bmatrix} b_{1i} & b_{2i} & b_{3i} & b_{4i} \end{bmatrix}$, $\mathbf{t} = \begin{bmatrix} t^3 & t^2 & t & 1 \end{bmatrix}^{\mathbf{T}}$ and k is the quarter of the fruit in the plane. Considering the symmetry planes, each eighth is symmetric to these planes. Coffee fruit geometries were designed in SolidWorks® software 2014 (Dassault Systèmes SolidWorks Corp., Waltham, MA, USA) applying the methodology described by Tinoco et al. [15], which included using digital images for the geometric reconstruction of the fruit, as shown in Figure 2b. The fruit models are the same obtained in the study carried out by Tinoco et al. [22]. Posteriorly, geometric models of the fruits will be used for harmonic finite element analysis.

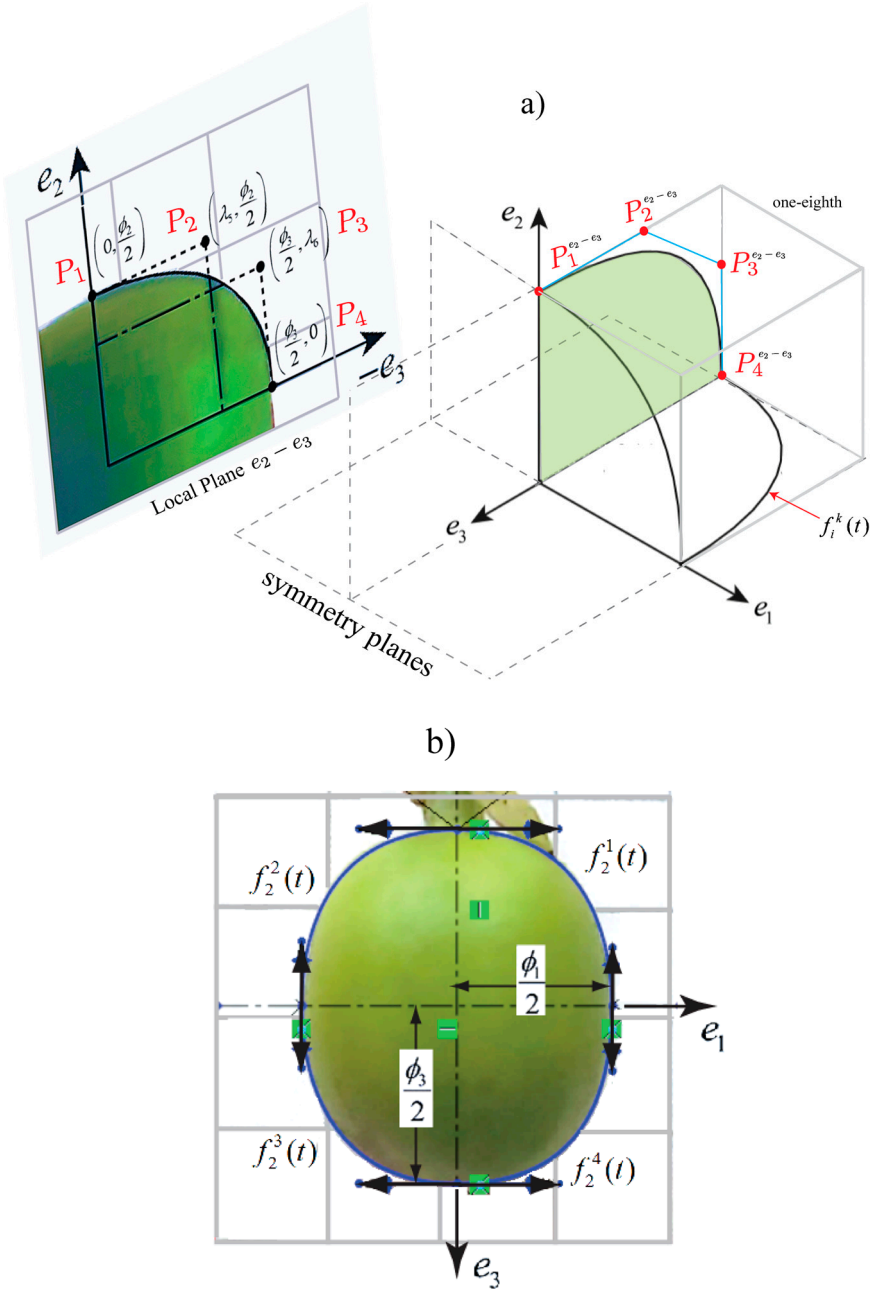

Figure 2. (**a**) Bezier curves defined for each eighth of the fruit. (**b**) Digital image to approximate the topology of the coffee fruit (case: unripe 220).

3. Physical-Mechanical Properties of the Fruit-Peduncle System of *Coffea arábica* L. var. Colombia

3.1. Density

The average density of coffee fruit *Coffea arábica* L. var. Colombia was measured by Ciro et al. [24], calculating the buoyancy force when the fruit was immersed in distilled water. It was determined in their study that the average density of the fruit is constant during ripening and its value is approximately 1.07 g/cm^3. For this study, we assumed that the density of the pedicel-peduncle structure is the same as the density of the coffee fruit.

3.2. Poisson's Ratio

In the study performed by Álvarez et al. [25], they determined Poisson's ratio by means of a method of digital pictures/picturing for the pedicel-peduncle structure. In their study, traction and compression forces were applied to samples and the deformation in points of reference was measured with digital images taken at a resolution of 58 pixels/mm. Table 1 shows Poisson's ratio for the pedicel-peduncle of coffee *Coffea arábica* in two ripening stages.

Table 1. Poisson's ratio for the structure pedicel-peduncle [25].

Stage	Poisson's Ratio	Standard Deviation
Unripe	0.3457	0.090
Ripe	0.3191	0.072

The value of Poisson's ratio had not been determined for a *Coffea arábica* L. var. Colombia fruit. However, the value is irrelevant in this study, since the fruit will not be submitted to external forces. This means that the fruit will not be subjected to considerable deformation amplitudes when these are compared with deformations of the pedicel-peduncle.

3.3. Young's Modulus

In the work performed by Carvajal-Herrera et al. [26], the firmness indexes of the *Coffea arábica* were experimentally determined, with K_1, K_2, and K_3 representing the firmness in the directions e_1, e_2, and e_3. Firmness refers to the stiffness of the fruit at the orthogonal directions, which depends on the geometry and the elastic properties. For our study, indices were approximated by analytical models using an optimization procedure (least square fitting) to estimate the parameters shown in Table 2. The determined models are illustrated in Figure 3 and listed in the first three columns. For firmness, we applied a dose-response function (BRF), which is expressed as:

$$y = A_1 + (A_2 - A_1)\left[\frac{p}{1+10^{(log(x_1)-x)h_1}} + \frac{1-p}{1+10^{(log(x_2)-x)h_2}}\right] \quad (2)$$

Additionally, Table 2 presents an approximation of Young's modulus of the *Coffea arabica* L. var. Colombia as a function of its ripening. The semi-empirical Young's modulus was determined by Tinoco [19] with a numerical approach from the firmness indices. The analytical model is included in the finite element analysis that will be performed in the next sections. The mathematical representation of Young's modulus is called Boltzmann Sigmoidal Model (BSE), which is described by the following equation:

$$y = \frac{A_1 - A_2}{1 + e^{(x-x_0)/dx}} + A_2 \quad (3)$$

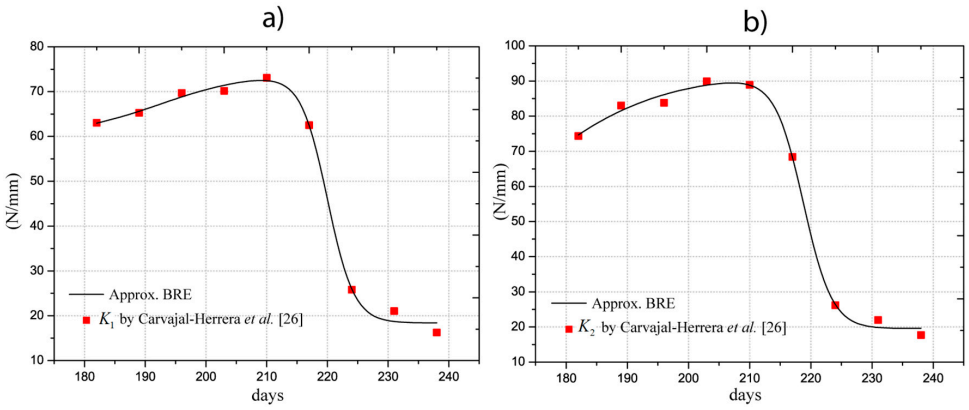

Figure 3. *Cont.*

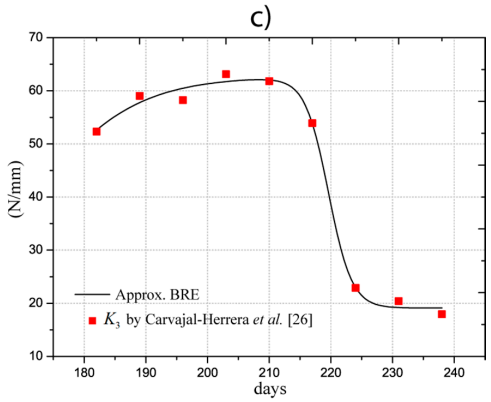

Figure 3. Firmness indices (**a**) K_1 (e_1); (**b**) K_2 (e_2); and (**c**) K_3 (e_3).

Table 2. Approximations of firmness indexes obtained by Carvaja-Herrera et al. [26] and Young's modulus approximated by finite element model (FEM).

Model BRF	BRF (N/mm) $(K_2 - \phi_2)$	BRF (N/mm) $(K_1 - \phi_1)$	BRF (N/mm) $(K_3 - \phi_3)$	Model BSE	BSE (E_f) (MPa)
A_1	4.042	19.765	19.116	A_1	18.844
A_2	74.382	25.750	19.837	A_2	5.654
$log(x_1)$	192.432	170.582	172.464	x_0	220.423
$log(x_2)$	220.019	218.810	219.636	dx	1.834
h_1	0.056	−0.038	−0.053	-	-
h_2	−0.198	−0.184	−0.230	-	-
p	0.204	−11.159	−59.427	-	-
Chi-square	6.53	8.49	5.80	Chi-square	0.758
R-square	0.988	0.991	0.984	R-square	0.98
Prob. > F (ANOVA)	1.6×10^{-3}	1.43×10^{-3}	1.88×10^{-3}	Prob. > F (ANOVA)	5.22×10^{-7}

The values of Young's moduli satisfy the firmness indexes in all orthogonal directions, meaning that the fruit is considered an isotropic material, as demonstrated by Tinoco et al. [15]. The estimations were obtained with convergence errors of firmness less than 5%. This requirement was included in the algorithm proposed by Tinoco et al. [15]. The determined values and the approximation are depicted in Figure 4 with red markers and a black line, respectively. The analytical model adjusted for the Young's modulus is described in Equation (3) and the values of the coefficients are listed in the fourth column of Table 2. The statistical approximation indicates that R^2 is 0.98 with a probability F much less than 5%. Therefore, the estimations of the models are in good correlation with the experimental and semi-empirical data.

In the ripening process, the fruit's Young's modulus varied during fruit growth, as evidenced in Figure 4. Starting from day 200, small changes in the Young's modulus manifested until day 210. From this day, variations in the elastic properties were visible, such that the fruit lost 62.80% of its initial Young's modulus by day 224. Subsequently, in the overripe stage 238, the fruit loses approximately 70% of its initial elastic capacity. In mechanical terms, the loss of elastic capacity means that the fruit has a greater probability of changing its shape if a low pressure is applied internally. As a result, the strains inside the fruit would increase easily. However, the biophysical phenomena are more complex inside the fruit as explained by Hall et al. [27]. However, these can be seen from a macro scale as consequences of biological complexities.

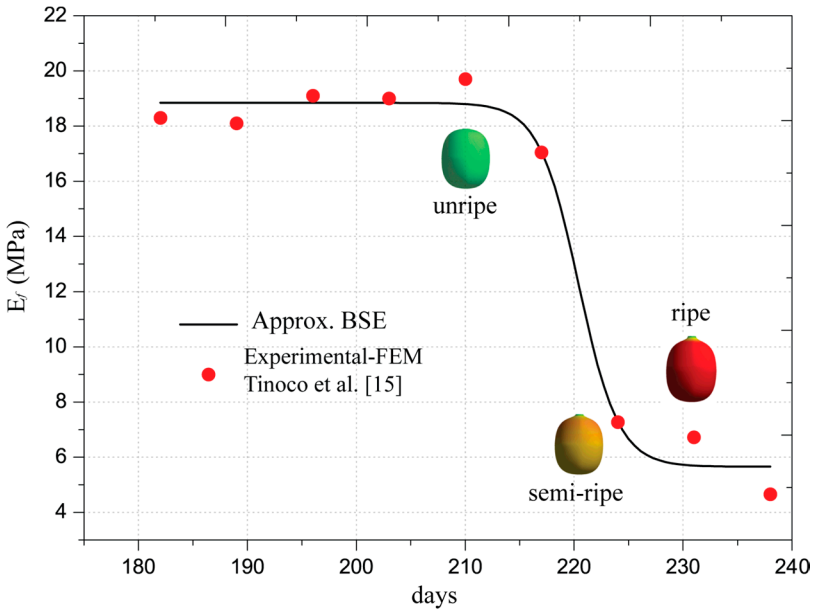

Figure 4. Approximated elastic modulus from FEM and Boltzmann Sigmoidal Model (BSE) model.

4. Finite Element Analysis of Fruit-Peduncle Structure

In this section, we present a finite element model (FEM) to study the stresses generated at the pedicel-fruit and pedicel-peduncle interfaces at different ripening stages. Analysis involved the application of a harmonic force on isolated coffee fruits as described in Figure 5. A computer SONY VAIO PC (M350 2.27 GHz i3 CPU, 8 GB RAM) with Windows 7 operating system was used to carry out a harmonic analysis in ANSYS® software version 14.5 (ANSYS Inc., Canonsburg, PA, USA). There were necessary computer aided design (CAD) models (geometric models) of fruit to define the finite element model. Five fruits were designed in the following stages: unripe 196, unripe 210, semi-ripe 224, ripe 231, and overripe 238. For each fruit model, geometry of the pedicel and peduncle was assumed to be cylindrical and was designed using the geometric data published by Álvarez et al. [28] and Martinez-Rodríguez et al. [25]. The deviation of the pedicel with respect to the peduncle was assumed to be 45°, since direction is irrelevant for the stiffness of the peduncle and the diameter was considered to be 2.11 mm. CAD models were drawn using SolidWorks® software 2014 (Dassault Systèmes SolidWorks Corp., Waltham, MA, USA) with the methodology outlined in Section 2, which was proposed by Tinoco et al. [15]. Elastic properties of the fruit and peduncle-pedicel are described in Section 5 and correspond to numerical approximation performed by Tinoco et al. [15]. As shown in Figure 5, kinematical considerations for the fruit-peduncle model are described by the following boundary conditions: (1) clamped at the point A and (2) free structures (fruit and pedicel). The fruit-pedicel and pedicel-peduncle interfaces are bonded and continuous. Different mesh types were used for the simulation of each structure. The selected elements were hexahedral for the pedicel and tetrahedral for the peduncle.

For the simulation, a harmonic force was applied to the fruit in the e_1 direction as shown in Figure 5. The applied force was $P = \left(2\hat{i} + 2\hat{j} + 2\hat{k}\right) \sin(\omega t)$ N, where ω is frequency. The application of the force was performed in a frequency range between 0 and 4000 Hz. With respect to the location of the force, it is known that dynamic excitations in frequency stimulate the natural behavior of the systems, independently of the location of forces, if the system satisfies the same boundary conditions. This statement is not true for nonlinear cases that include friction and vibro-impact among others. In the case of any external force applied constantly on the fruit, the stress values will be different in the interfaces of the fruit and peduncle. However, these will have a qualitative sense in our study, since the aim was to show that there are frequency intervals where ripe fruits can be dynamically stimulated without affecting the unripe fruits. For harmonic stress analysis, the stresses were be determined at the interfaces of the pedicel (inferior and superior) with the following stress intensity determined by the following expression:

$$\sigma_i = \sigma_{p(Max)} - \sigma_{p(Min)} \tag{4}$$

where $\sigma_{p(Max)}$ is the maximum principal stress and $\sigma_{p(Min)}$ is the minimum principal stress. It is important to point out that the stresses were be obtained at the edge of the inferior and superior interfaces of the pedicel as described in Figure 5.

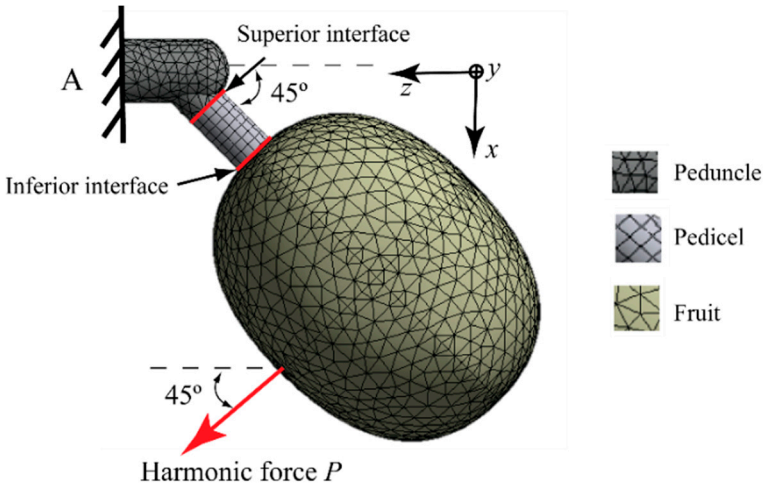

Figure 5. Finite element mesh model for the fruit-peduncle system (ripe 231 days after anthesis DAA).

5. Results and Discussion

Figure 6a,b show the stresses generated at the pedicel interfaces by the harmonic force applied in the frequency interval of 0–400 Hz. The force was applied on fruits in different ripening stages (189, 210, 217, 224, 231, and 224 DAA), the ripening is measured in days after anthesis (DAA). Colors represent each ripening stage and the highlighted red line indicates the ripe fruit (231 DAA). We observed that, for each ripening stage, just three peaks appeared in all frequency bandwidths, which corresponded to the natural resonances. It was indicated that, for each natural frequency, kinematics associated to the resonance exists, which is called vibration mode or shape. It is important to point out these dynamic characteristics because they are considered in the analysis.

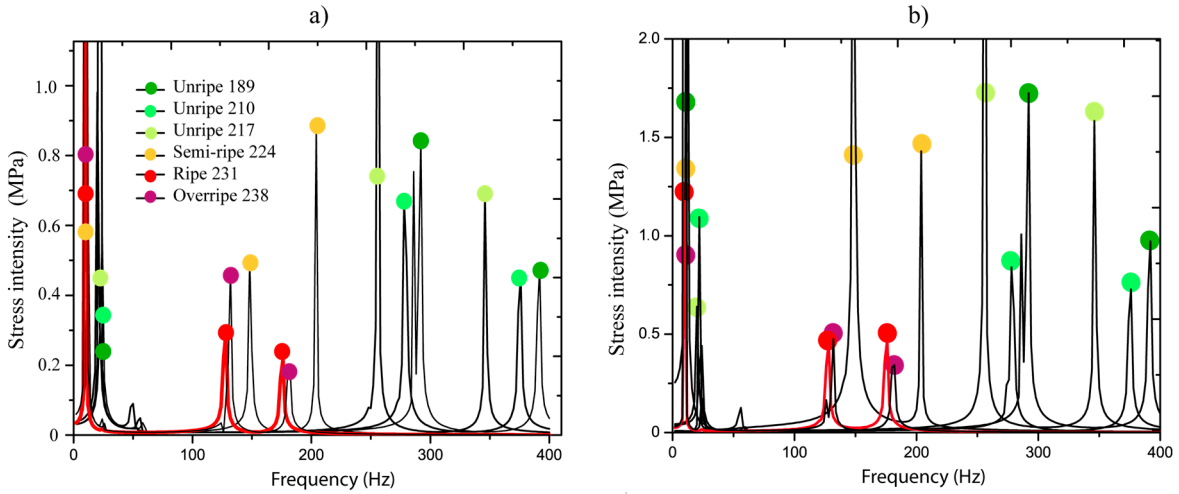

Figure 6. *Cont.*

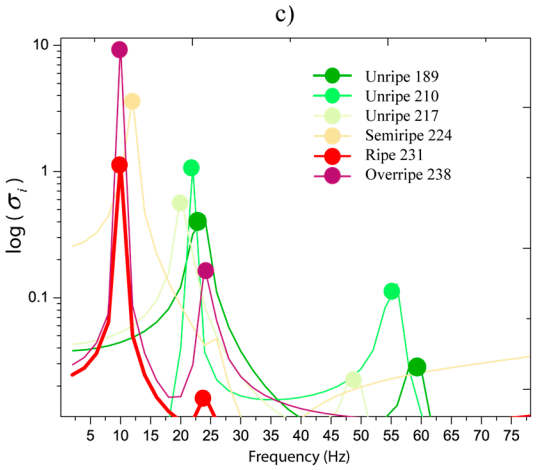

Figure 6. Stress intensity in the frequency spectrum: (**a**) inferior interface, (**b**) superior interface, and (**c**) interval 2.5–80 Hz at the inferior interface.

Figure 6c demonstrates that stresses are greater when the ripening is close to the overripe state in the first resonance frequency. Basically, the stress values oscillated in 0.2 and 1 MPa in the unripe state from 189 to 217 DAA. When ripe, 224 to 238 DAA, the stress values are between 1 to 10 MPa. We observed that resonances in 5–30 Hz are very close. This indicates that if a system with various fruits in different ripening stages is excited, all fruits will be stimulated and this is not favorable for selective harvesting purposes. The main idea is that fruits in ripe stages are dynamically stimulated.

In Figure 6a,b, the behavior of resonances 2 and 3 are analyzed, respectively. We determined that when the fruit is in any ripening stage, the ratio ω_2/ω_3 between the natural frequencies has a mean of 73.7% with a standard deviation of 0.93%. This means that the natural frequency 2 represents 73.7% of natural frequency 3 in all ripening stages. The relationship shows that when the natural frequency 2 is moving to the left (ripening process), the ratio ω_2/ω_3 stays constant.

Figure 6a,b show that the stress values in natural frequency 2 are greater than those produced in the third resonance in the majority of cases. Therefore, a higher detachment impact over the interfaces (pedicel-peduncle and pedicel-fruit) can be produced by the dynamics of resonance 2. Further, we observed that the natural frequencies 2 and 3 were isolated for the ripe fruit at 231 DAA (red line) of the others frequencies, which correspond to unripe stages (lower than 231 DAA).

This defines the existence of a dynamic stimulus inside the interval 100 to 200 Hz that can directly excite only ripe fruits.

To prove clearly how the natural frequencies 2 and 3 move with respect to the ripening days, two models were approximated using the Boltzmann Sigmoidal Model (BSE) in Equation (3). The constants of the models are listed in Table 3 and the model is plotted in Figure 7. The approximations fit with a good accuracy since the correlation R was close to 1 and the F is less than 0.05 in ANOVA.

Table 3. Approximations of modal shape 2 and 3 using the Boltzmann Sigmoidal Model (BSE) model.

Modal Shape	2	3
A_1	285.86	383.11
A_2	129.53	178.38
x_0	219.91	220.03
dx	2.053	2.053
Chi-square	46.48	97.90
R^2	0.99	0.99
Prob. > F	6.54×10^{-4}	7.56×10^{-4}

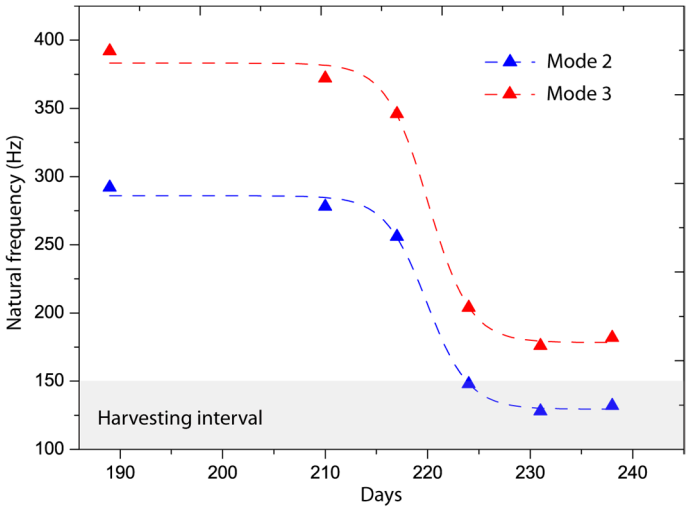

Figure 7. Curves of approximations for natural frequencies respect to ripening days.

The curves in Figure 7 illustrate that both natural frequencies follow the elastic model of the fruit, since it has the same behavior as shown in Figure 2. Basically, the results imply that the natural frequencies decrease as fruit ripening increases. For the analysis, the frequency interval 120–150 Hz was chosen and is shown in Figure 7 in gray. In this interval, fruits could be stimulated in the ripening stages 224–238 DAA without any dynamic interference with the other ripening stages. In the case of natural frequency 3, the frequency interval was delimited by 170 to 210 Hz. Nevertheless, if there was excitation in vibration mode 3, the fruits in ripening stages in 220–223 DAA are also excited. Therefore, the frequency range 120 to 150 Hz is better to only stimulate the resonance 2; it was shown to be a feasible frequency spectrum for selective harvesting. Notably, any system coupled to the peduncle, such as a branch will not affect the resonance, since in theory, these will also be coupled in the whole system.

Maximum principal stresses and principal vectors were determined from the simulation to differentiate the stresses generated at the pedicel interfaces, as illustrated in Figure 8, where the principal vectors for vibration modes 2 and 3 are shown. In Figure 8a, the stresses generate a bending state in vibration mode 2, since there are fibers under tension (red arrows) and compression (blue arrows) at the same time. This behavior provides a great advantage from a dynamic point of view because the stresses are concentrated at the pedicel-fruit and the pedicel-peduncle joints. Figure 8a

describes the values of the maximum principal stresses that reached a maximum value of 5.03 Mpa for mode 2 using a color scale. In reality, these stresses should overcome the failure stresses of the pedicel fibers to detach the coffee fruit.

In Figure 8b, the principal directions of mode 3 are analyzed; these act under tension or compression, at the same time producing shear stresses. Maximum principal stresses achieved 0.2 MPa at the interfaces, which are lower than the stress intensity of mode 2 (bending state). The strength properties at the interfaces define the detachment rules and these can be experimentally determined for any variety of coffee fruit.

Vibration shapes were computed as shown in Figure 9. The motion refers to the displacements that the fruits experience in resonances 2 and 3. For mode 2, we observed that the principal motion causes pedicel bending, since the fruit tends to rotate as explained by the stress analysis. The maximum amplitude of the displacement was reached at the pedicel-fruit interface, achieving a maximum value of 2.6 mm. This bending motion helps to produce a failure mechanism at the interfaces. Further, it can be seen that a point of zero motion was evidenced in the fruit, which is demarked in the graph in blue. It implies that the fruit has two points of pivot that promote the rotation of the fruit-peduncle system.

Figure 9b shows the motion of vibration mode 3. In this mode, fruit follows an axial motion with a small rotation that generates shear stress at the pedicel and bending in the peduncle. The maximum displacement achieved by the fruit was 0.07 mm; this value is very small compared with the displacement obtained in mode 2. According to the analysis performed, the frequency spectrum of 120 to 150 Hz for purposes of selective harvesting is presented as a feasible interval for stimulating the detachment of ripe fruits.

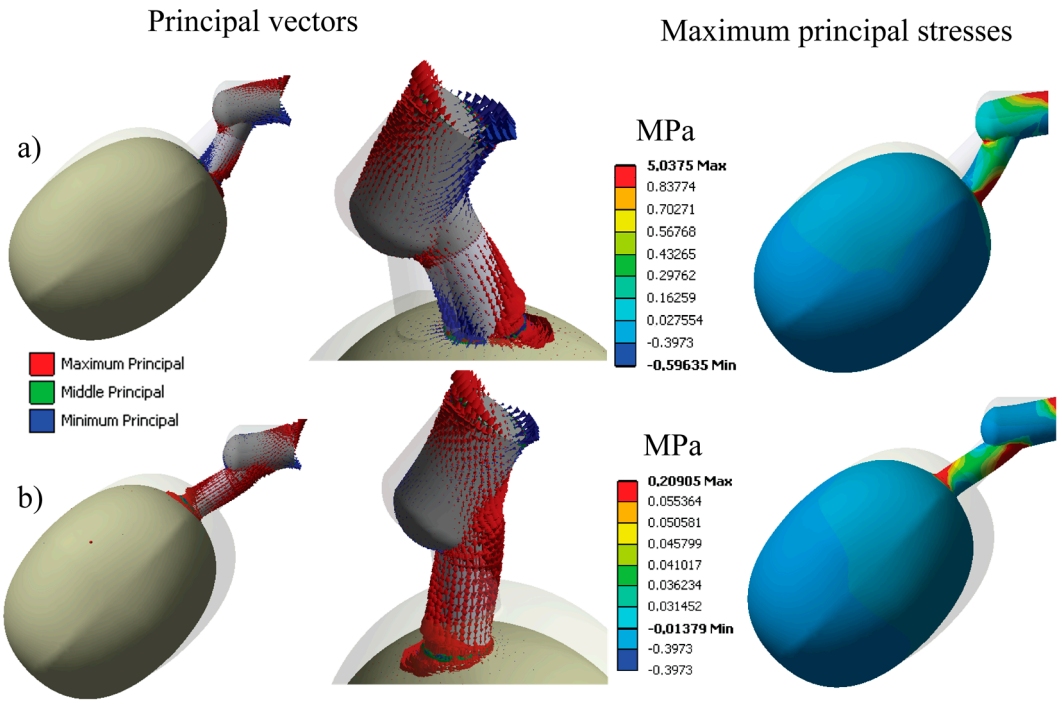

Figure 8. Principal vectors and maximum principal stresses for the fruit at time of ripening at 231 DAA. (**a**) Vibration mode 2; (**b**) vibration mode 3.

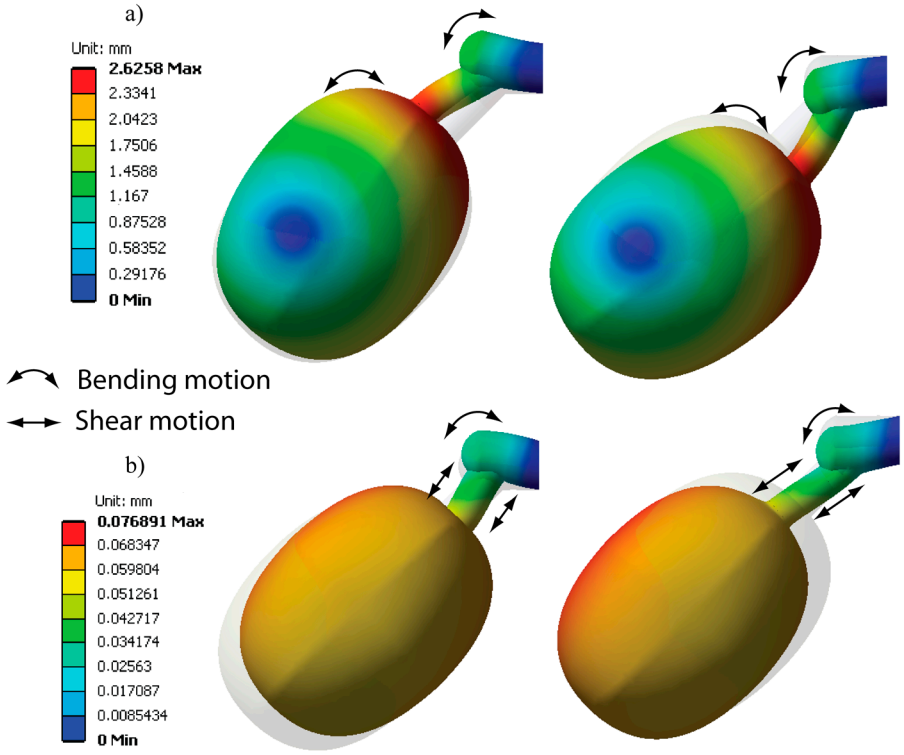

Figure 9. Ripe fruit at 231 DAA. (**a**) Displacement field in 128 Hz, vibration mode 2. (**b**) Displacement field in 182 Hz, vibration mode 3.

6. Conclusions

A harmonic stress analysis was performed to evaluate the stress intensity at the pedicel-fruit and pedicel-peduncle interfaces of *Coffea arabica* L. var. Colombia. Three vibration modes were identified in the frequency spectrum of 0–400 Hz by means of a finite element analysis. We observed that natural frequencies decreased when fruit ripening increased. For purposes of selective harvesting, the natural frequency 2 (128 Hz) proved suitable in its dynamic behavior, since the fruit-pedicel-peduncle system experienced bending motions. We analyzed that the dynamic excitation between 120 and 150 Hz could help selectively detach ripe fruits according to the numerical results. These results show that dynamic stimulus of the coffee tree should be completed in frequencies between 100 and 200 Hz. Finally, the findings of this study should be verified experimentally.

Author Contributions: Conceptualization, H.A.T.; methodology, H.A.T. and F.M.P.; validation, H.A.T. and F.M.P.; formal analysis, H.A.T. and F.M.P.; investigation, H.A.T. and F.M.P.; writing—original draft preparation, H.A.T.; writing—review and editing, H.A.T. and F.M.P.

Funding: This research received no external funding.

Conflicts of Interest: The authors declare no conflict of interest.

References

1. Restuccia, D.; Spizzirri, U.G.; Parisi, O.I.; Cirillo, G.; Picci, N. Brewing effect on levels of biogenic amines in different coffee samples as determined by LC-UV. *Food Chem.* **2015**, *175*, 143–150. [CrossRef] [PubMed]
2. Sanz, C.G.C.; Mejía, C.V.; García, E.C.; Torres, J.S.A.; Calderón, E.Y.T. *El Mercado Mundial del café y su Impacto en Colombia (No. 7102012)*; Banco de la República: Bogotá, Colombia, 2012; Available online: http://www.banrep.org/docum/Lectura_finanzas/pdf/be_710.pdf (accessed on 17 September 2018).
3. Lopez-Fisco, H.A.; Rodriguez-Gómez, C.A.; Oliveros-Tascón, C.E.; Sanz-Uribe, J.R. Aroandes, una tecnología para la cosecha manual de café con alta calidad. *Cenicafé* **2008**, *59*, 283–294.

4. Peterson, D.L.; Wolford, S.D. Mechanical harvester for fresh market quality stemless sweet cherries. *Trans. ASAE* **2001**, *44*, 481–485. [CrossRef]
5. Peterson, D.L. Harvest mechanization progress and prospects for fresh market quality deciduous tree fruits. *HortTechnology* **2005**, *15*, 72–75.
6. Ferguson, L.; Rosa, U.A.; Castro-Garcia, S.; Lee, S.M.; Guinard, J.X.; Burns, J.; Glozer, K. Mechanical harvesting of California table and oil olives. *Adv. Hortic. Sci.* **2010**, *24*, 53–63.
7. Tombesi, S.; Poni, S.; Palliotti, A.; Farinelli, D. Mechanical vibration transmission and harvesting effectiveness is affected by the presence of branch suckers in olive trees. *Biosyst. Eng.* **2017**, *158*, 1–9. [CrossRef]
8. Barbosa, J.A.; Salvador, N.; Silva, F.M. Desempenho operacional de derriçadoras mecânicas portáteis, em diferentes condições de lavouras cafeeira. *Revista Brasileira de Engenharia Agrícola e Ambiental* **2005**, *9*, 129–132. [CrossRef]
9. Oliveira, E.; Silva, F.M.; Salvador, N.; Souza, Z.M.; Chalfoun, S.M.; Figueiredo, C.A.P. Custos operacionais da colheita mecanizada do cafeeiro. *Pesquisa Agropecuária Brasileira* **2007**, *42*, 827–831. [CrossRef]
10. Coelho, A.L.D.F.; Santos, F.L.; Pinto, F.A.; de Queiroz, D.M. Determinação das propriedades geométricas, físicas e mecânicas do sistema fruto-pedúnculo-ramo do cafeeiro. *Revista Brasileira de Engenharia Agrícola e Ambiental* **2015**, *19*, 286–292. [CrossRef]
11. Mbuge, D.O.; Langat, P.K. Principles of a mechanical shaker for coffee harvesting. *Agric. Eng. Int. CIGR J.* **2008**, *10*. Available online: http://cigrjournal.org/index.php/Ejounral/article/viewFile/1007/1000 (accessed on 17 September 2018).
12. Castillo-Ruiz, F.J.; Tombesi, S.; Farinelli, D. Tracking olive fruit movement and twisting during the harvesting process using video analysis. *Acta Hortic.* **2018**, *1199*, 409–414. [CrossRef]
13. Ciro, H.J.; Oliveros-Tascon, C.E.; Álvarez, F. Estudio dinámico bajo oscilación forzada del sistema fruto-pedúnculo (SFP) del café variedad Colombia. *Revista Facultad Nacional de Agronomía* **1998**, *51*, 63–90.
14. Gaskin, E.; Martínez, A.; Llanes, O. Búsqueda de modos de vibración apropiados para la cosecha selectiva del café. *Revista Ciencias Técnicas Agropecuarias* **2007**, *16*, 1–6.
15. Tinoco, H.A.; Ocampo, D.A.; Peña, F.M.; Sanz-Uribe, J.R. Finite element modal analysis of the fruit-peduncle of *Coffea arabica* L. var. Colombia estimating its geometrical and mechanical properties. *Comput. Electron. Agric.* **2014**, *108*, 17–27. [CrossRef]
16. Tsatsarelis, C.A. Vibratory olive harvesting: The response of the fruit-stem system to fruit removing actions. *J. Agric. Eng. Res.* **1987**, *38*, 77–90. [CrossRef]
17. De Oliveira, E.; da Silva, F.M.; Salvador, N.; Figueiredo, C.A.P. Influência da vibração das hastes e da velocidade de deslocamento da colhedora no processo de colheita mecanizada do café. *Engenharia Agrícola* **2007**, *27*, 714–721. [CrossRef]
18. Santos, F.L.; de Queiroz, D.M.; Pinto, F.D.A.; de Resende, R.C. Efeito da frequência e amplitude de vibração sobre a derriça de frutos de café. *Revista Brasileira de Engenharia Agrícola e Ambiental* **2010**, *14*, 425–431. [CrossRef]
19. Álvarez-Mejía, F.; Oliveros-Tascón, C.E.; Sanz-Uribe, J.R. Evaluation of Mechanical Beaters in Coffee Harvesting. *Revista Facultad Nacional de Agronomía* **2013**, *66*, 6919–6928.
20. Coelho, A.L.D.F.; Santos, F.L.; Pinto, F.D.A.; Queiroz, D.M.D. Detachment efficiency of fruits from coffee plants subjected to mechanical vibrations. *Pesquisa Agropecuária Tropical* **2015**, *45*, 406–412. [CrossRef]
21. Coelho, A.D.F.; Santos, F.L.; de Queiroz, D.M.; Pinto, F.D.A. Dynamic behavior of the coffee fruit-stem-branch system using stochastic finite element method. *Coffee Sci.* **2016**, *11*, 1–10.
22. Tinoco, H.A.; Peña, F.M. Harmonic stress analysis on *Coffea arábica* L. var. Colombia fruits in order to stimulate the selective detachment: A finite element analysis. *Simulation* **2017**, *94*, 163–174. [CrossRef]
23. Tinoco, H.A. Modeling Elastic Geometric Properties of *Coffea arabica* L var Colombia Fruits by an Experimental-numerical Approach. *Int. J. Fruit Sci.* **2017**, *17*, 159–174. [CrossRef]
24. Ciro, H.J.; Álvarez, F.; Oliveros, C.E. Estudio experimental de la dinámica de las vibraciones longitudinales y transversales aplicadas a las ramas de café. *Revista Facultad Nacional de Agronomía* **1998**, *51*, 245–275.
25. Martinez-Rodríguez, A.; de Queiroz, D.M.; Espinosa, B.G.; Zandonadi, R. Determinación de propiedades físico-mecánicas de los frutos de café (*Coffea arábica* variedad Catuai) relacionadas con la cosecha mecanizada. *Revista Ciencias Técnicas Agropecuarias* **2006**, *15*, 22–27.

26. Carvajal-Herrera, J.J.; Aristizabal-Torres, I.D.; Oliveros-Tascón, C.E.O. Evaluación de propiedades físicas y mecánicas del fruto de café (*coffea arabica* L. var. Colombia) durante su desarrollo y maduración. *Dyna* **2012**, *79*, 173.
27. Hall, A.J.; Minchin, P.E.; Clearwater, M.J.; Génard, M. A biophysical model of kiwifruit (*Actinidia deliciosa*) berry development. *J. Exp. Bot.* **2013**, *64*, 5473–5483. [CrossRef] [PubMed]
28. Álvarez, E.; Álvarez, F.; Oliveros, C.E.; Montoya, E.C. Propiedades físico-mecánicas del fruto y del sistema fruto-pedúnculo del café variedad Colombia. *Revista Facultad Nacional de Agronomía* **1999**, *52*, 701–720.